Supporting information

Time-gated ratiometric detection with the same working wavelength to minimize the interferences from photon attenuation for accurate in vivo detection

Shengming Cheng,† Bin Shen,† Wei Yuan,† Xiaobo Zhou,† Qingyun Liu, †Mengya Kong,† Yibing Shi, † Pengyuan Yang, † Wei Feng,†* and Fuyou Li†*

† Institutes of Biomedical Sciences & Department of Chemistry & State Key Laboratory of Molecular Engineering of Polymers, Fudan University, 220 Handan Road, Shanghai 200433, P.R. China

* Correspondence should be addressed to W. F. (fengweifd@fudan.edu.cn) and F.Y.L. (fyli@fudan.edu.cn).

Experimental Section

Materials: All reagents and chemicals were obtained from commercial supplies. Rare earth oxides RE_2O_3 (99.999%) (RE^{3+}=Y^{3+}, Nd^{3+}) were purchased from Shanghai Yuelong New Materials Co. Ltd. Octadecene (ODE) (>90%) and oleic acid (OA) (>90%) were purchased from Sigma-Aldrich. Ethanol and cyclohexane were purchased from Adamas-beta Reagent. $RECl_3$ were prepared with the reported method dissolving the corresponding oxides in hydrochloric acid at elevated temperature and removing the solvent. All other chemical reagents of analytical grade were used directly without further purification. Balb/c mice (4 weeks) were purchased from the Second Military

Medical University and were housed under standard environmental conditions. Animal procedures were in agreement with the guidelines of the Institutional Animal Care and Use Committee.

Instruments: X-ray powder diffraction (XRD) measurements were performed on a Bruker D8 diffractometer in the 2θ range of 10- 90^{o}. Fluorescence emission spectra were measured on an Edinburgh FLS920 luminescence spectrometer. UV-Vis absorption spectra were performed on a Lambda 35 spectrophotometer. Transmission electron microscope (TEM) messages were collected on a JEM 2010 operating at an acceleration voltage of 200 kV. Dynamic light scattering was tested in the NanoZS90. ICP-AES was tested in the iCAP 7400.

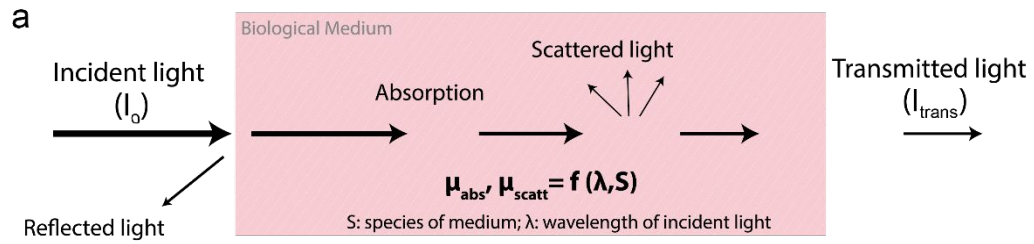

The intensity could be derived from radiance by integration over the solid angle as follows:

$$I(r) = \int_{4\pi} J(r,s) s d\omega \tag{1}$$

where J (r, s) is the radiance.

In photon transport theory, the radiative transport equation is as follows:

$$\frac{dJ(r,s)}{ds} = -\mu_t J(r,s) + \frac{\mu_s}{4\pi} \int_{4\pi} p(s,s') J(r,s') d\omega' \tag{2}$$

where p (s, s') is the phase function of a photon scattered from direction s' into s, ds is an infinitesimal path length, and dω' is the elementary solid angle about the direction s'.

On the other hand, the radiance inside a turbid medium can be divided into a coherent and a diffuse term according to the following relationship

$$J = J_c + J_d \tag{3}$$

where Jc is coherent radiance and Jd is diffuse radiance.

When the diffuse term is noticeably smaller than the coherent term Jc+Jd≈Jc， the intensity at a distance z from the tissue surface could be given by Lambert's law (First-Order Scattering) as follows:

$$I(z) = I_0 \exp[-(\mu_a + \mu_s)z] \tag{4}$$

When the scattering overwhelms the absorption, we could expand the diffuse radiance Jd in a series by[1]

$$J_d = 1/4\pi(I_d + 3Fds + \ldots) \tag{5}$$

where Id is the diffuse intensity, and the vector Fd is determined by

$$F_d(r) = \int_{4\pi} J_d(r,s) s d\omega \tag{6}$$

In general, the diffusion approximation thus states that

$$I = I_c + I_d = A \exp(\mu_t z) + B \exp(\mu_{eff} z),\ A+B=I_0 \tag{7}$$ [2]

where $\mu_t = \mu_a + \mu_s$ and $\mu_{eff} = [3\mu_a\mu_t(1-g)]^{1/2}$, g is the scattering anisotropy factor.

Figure S1. Schematic illustration of light transmitting into biological tissue.

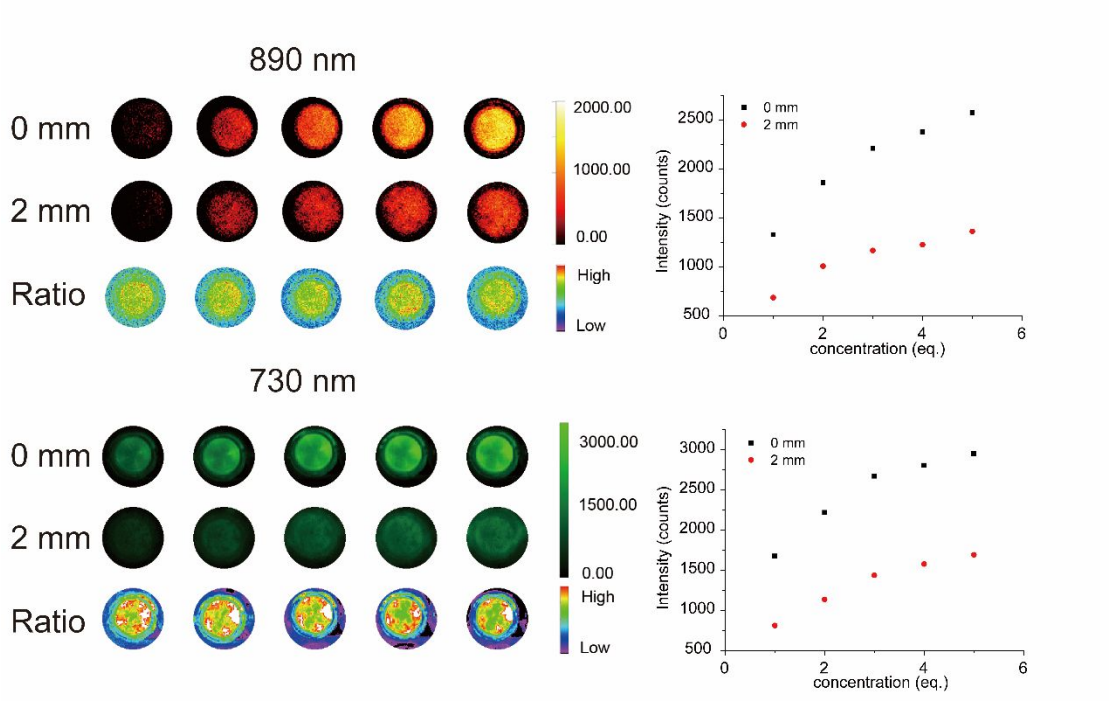

Figure S2. Images of light (730 nm and 890 nm) through 0 mm and 2 mm pork. the intensity of light with different wavelength (730 nm and 890 nm) undergone significant attenuation after transmitting 2 mm pork. But both of the k values of two groups did not change within the range of light intensity we measured (the ratio of I_{em} to I_{em}^{trans} is k).

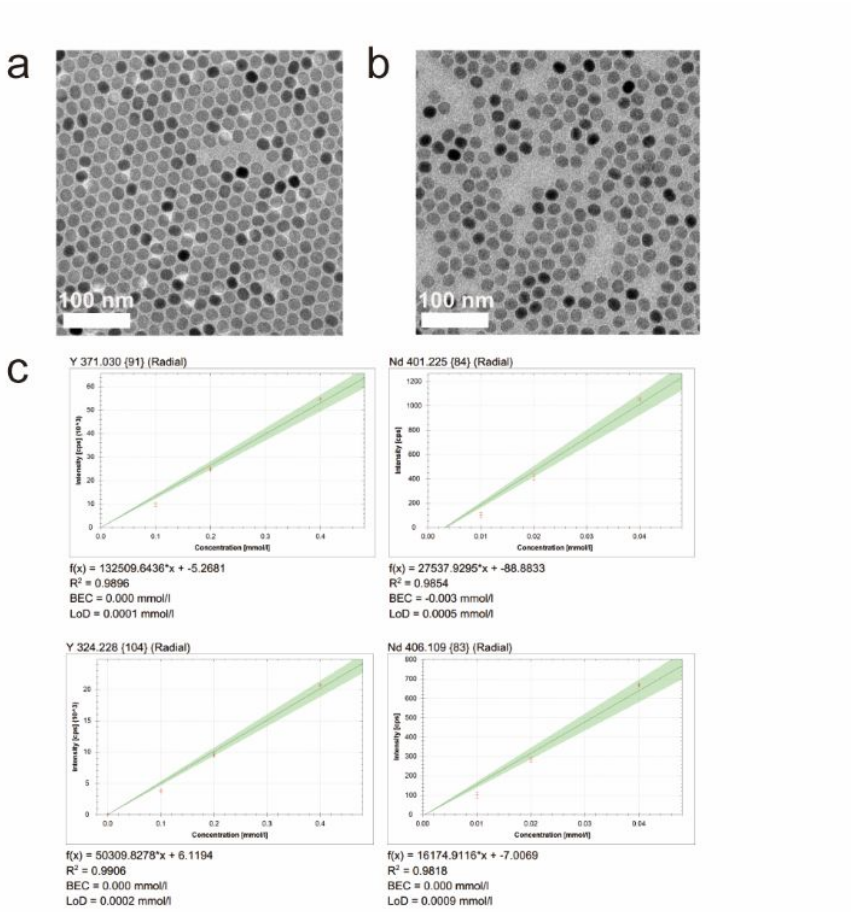

	Concentration average	Concentration RSD
Y 371.030 {91} (Radial)	0.429 mmol/l	2.0 %
Nd 401.225 {84} (Radial)	0.023 mmol/l	7.8 %
Y 324.228 {104} (Radial)	0.428 mmol/l	2.0 %
Nd 406.109 {83} (Radial)	0.023 mmol/l	8.4 %

Figure S3. TEM image of $NaYF_4$:Nd (a) and $NaYF_4$:Nd@Cy860@PC (b), bar=100 nm. (c) The concentration and composition of Nd^{3+} and Y^{3+} ions measured by ICP-AES. The ratio of actual doped Nd^{3+} ions is ~5.1%.

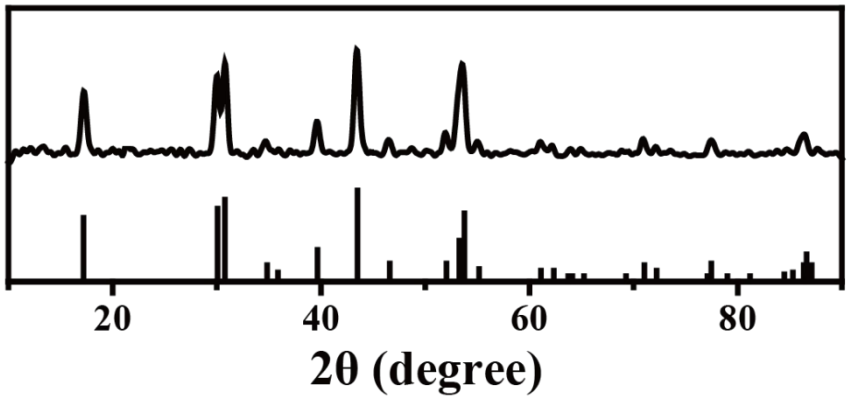

Figure S4. XRD patterns of OA- $NaYF_4$: Nd (JCPDS no.16-0334).

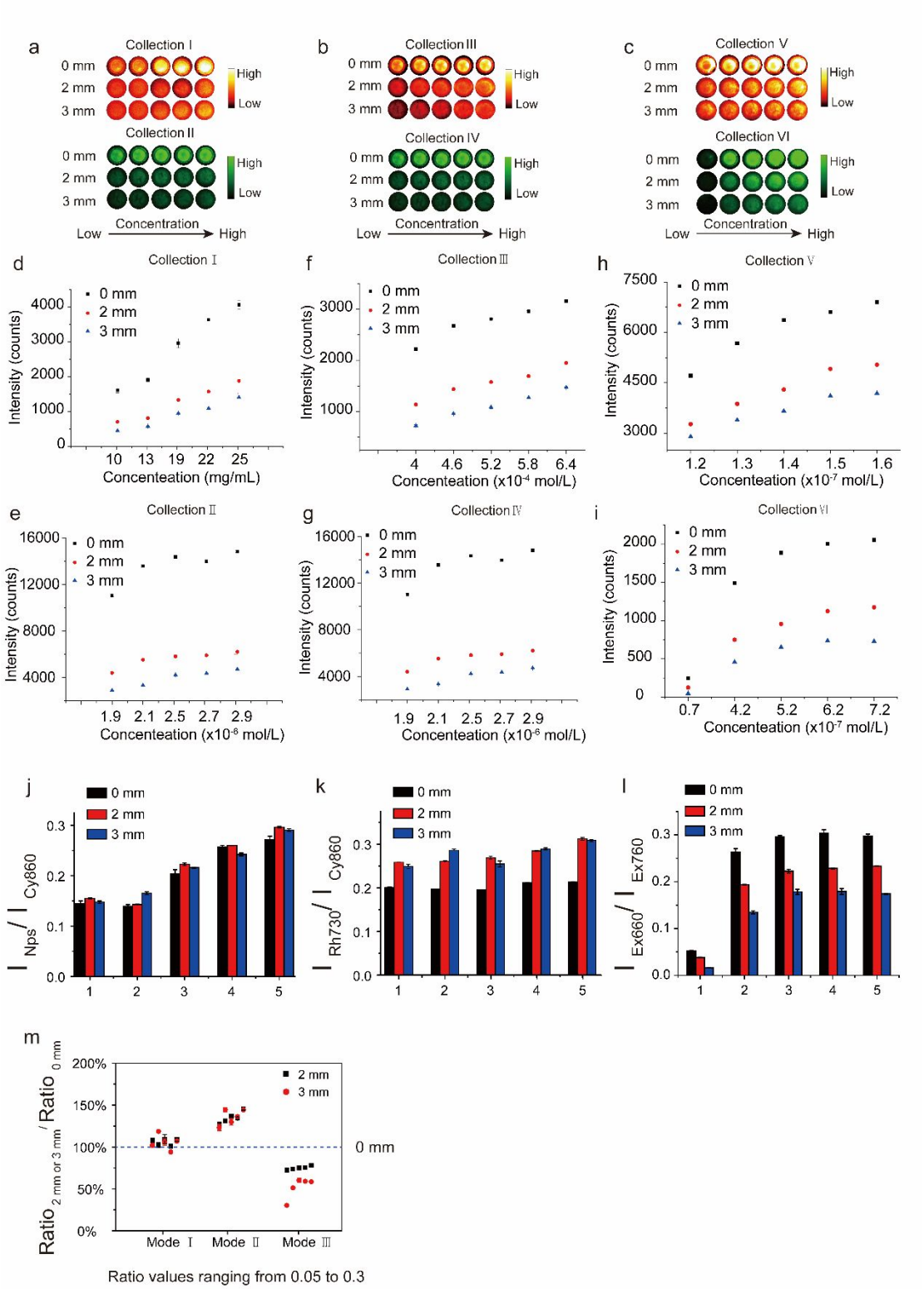

Figure S5. (a-c) Imaging pictures of six collection windows in which four types of emissive materials with different concentration are covered with different thick pork.

(d-i) Emission intensities of imaging pictures(a-c) (j-l) The ratio values of three imaging modes (the intensities in collection window I, III, VI to the intensities in collection window II, IV, V. (m) The deviations between the ratio signals measured with pork blocking and ratio signals without pork blocking in three modes when the ratio signals ranged from 0.05 to 0.3.

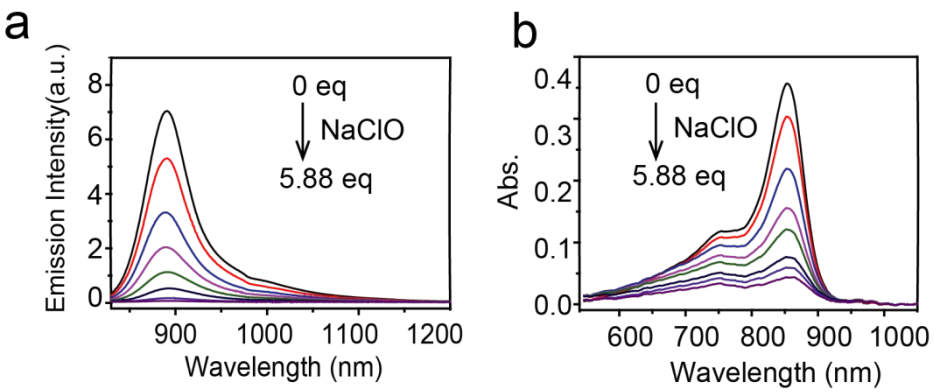

Figure S6. Changes in absorption spectra (a) and fluorescence emission spectra (b) of 2.7 μM solution of Cy860 upon gradual addition of NaClO.

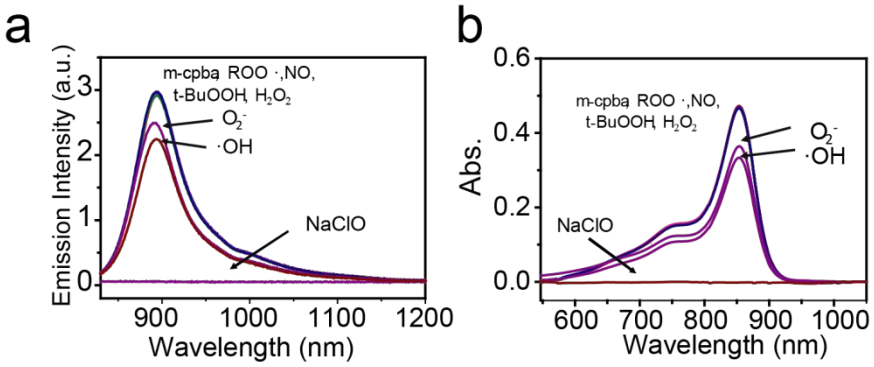

Figure S7. Changes in absorption spectra (a) and fluorescence emission spectra (b) of 3.5 μM solution of Cy860 upon gradual addition of NaClO, m-cpba, H_2O_2, ·OH, NO, O_2^-, ROO·, tBuOOH.

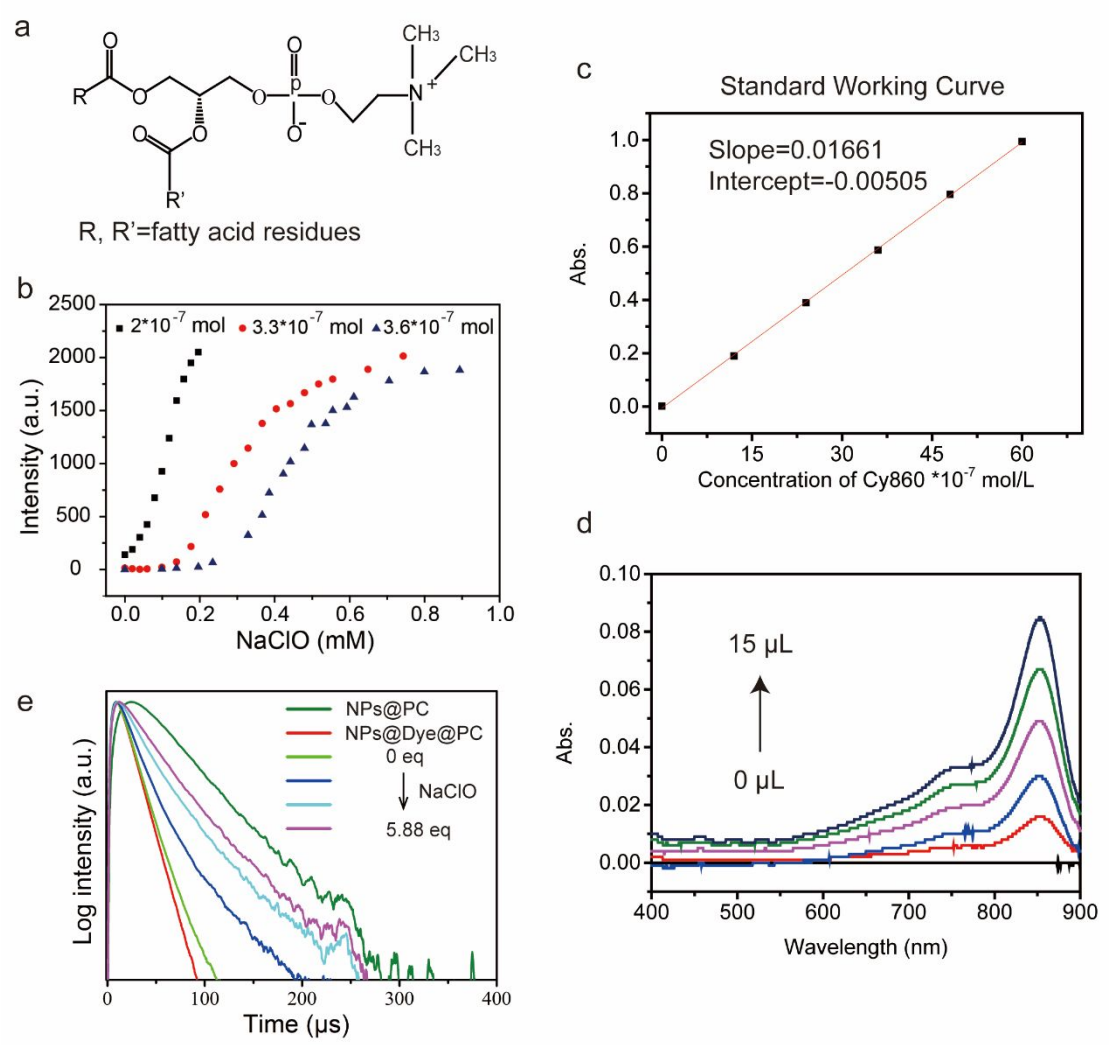

Figure S8. (a) The structural formula of PC. (b) Changes in emission intensity of nanoparticles in nanosystem (OA- $NaYF_4$: Nd-0.1 mmol, Cy860-2*10 $^{-7}$ mol, 3.3*10 $^{-7}$ mol, 3.6*10 $^{-7}$ mol) upon gradual of NaClO tested in TG imaging system with time-gating unit on. (c) The standard working curve of Cy860 in the mixture of EtOH and H_2O (v/v: 1:1). (d) Changes in absorption spectra of the mixture of EtOH and H_2O (v/v: 1:1) upon gradual addition of the supernatant (0, 3, 6, 9, 12, 15 μL; the total volume of the supernatant is 2.5 mL). (e) Changes of lifetime of Nd^{3+} ions (ex: 808 nm, em: 893 nm) upon gradual addition of NaClO.

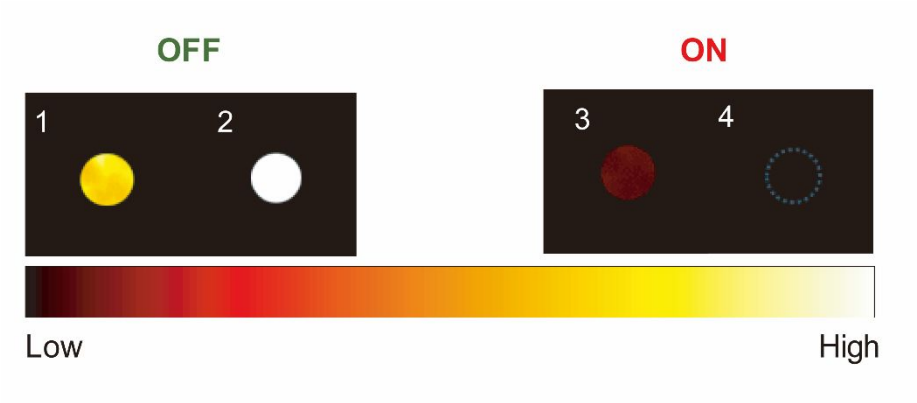

Figure S9. Fluorescence images of Cy860 (2,4) and $NaYF_4$:5%Nd (1,3) in TG imaging system with time-gating unit on (3,4) and off (1,2).

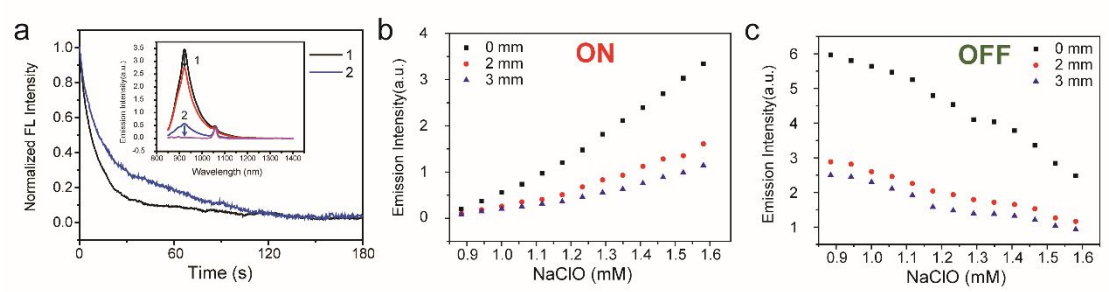

Figure S10. (a) With the addition of NaClO ($1*10^{-7}$ mol) to composite probe unencapsulated with different amount of Cy860 (1, $NaYF_4$: Nd: 0.3 mmol, Cy860: $0.62*10^{-7}$ mol; 2, $NaYF_4$: Nd: 0.3 mmol, Cy860: $0.12*10^{-7}$ mol), the luminescence of Cy860 decreased. And 3-min was enough for the full reaction. (b-c) The fluorescence intensity of $NaYF_4$: Nd@Cy860@PC (0.3 mmol) system in the aqueous solution upon gradual addition of sodium hypochlorite (from 0.88 to1.58 mmol/L, 300 μL in total) measured through tissue of 0 mm, 2 mm, 3 mm (power density:530 mw/cm^2). ON state: gain 10, exposure time 5s, duty cycle 40%, phase position:15°. OFF state: gain 2, exposure time 1s.

I_{ON}/I_{OFF}	0 mm (A)	2 mm (B)	|(B-A)/A|	3 mm (C)	|(C-A)/A|
1	0.34183	0.34324	0.004125	0.31381	0.081971
2	0.64457	0.6516	0.010906	0.60131	0.067115
3	0.99303	0.99337	0.000342	0.88444	0.109352
4	1.34819	1.43316	0.063025	1.20789	0.104065
5	1.85131	1.79823	0.02867	1.62992	0.119586
6	2.51669	2.49679	0.00791	2.2788	0.094525
7	3.25992	3.50002	0.073652	3.11283	0.045121
8	4.43312	4.63167	0.044788	3.9908	0.099776
9	5.24274	5.42328	0.034436	4.56161	0.129919
10	6.32669	6.79805	0.074503	5.71189	0.097176
11	8.0197	8.39174	0.046391	7.34272	0.084415
12	10.66764	10.68116	0.001267	9.52628	0.106993
13	13.48005	13.84488	0.027064	12.25268	0.091051
Pearson's r		0.9994		0.9997	
Average			0.0321		0.0947

Figure S11. the ratio values measured through pork (0 mm, 2 mm, 3 mm), the relative deviations and the Pearson correlation coefficient between ratios measured through tissue (2 mm and 3 mm) and ratios measured through tissue of 0 mm.

Equation	y = Intercept + B1*x^1 + B2*x^2 + B3*x^3 + B4*x^4		
Weight	No Weighting		
Residual Sum of Squares	0.21962	0.2179	0.15164
Adj. R-Square	0.99837	0.99846	0.99862
		Value	Standard Error
0 mm	Intercept	167.97593	70.12377
	B1	-601.34476	235.79717
	B2	798.54452	293.63162
	B3	-468.695	160.54481
	B4	104.42448	32.53344
2 mm	Intercept	180.79308	69.84937
	B1	-637.5235	234.87448
	B2	833.83936	292.48262
	B3	-482.24281	159.91659
	B4	106.01641	32.40614
3 mm	Intercept	177.52857	58.26894
	B1	-632.38832	195.93431
	B2	835.48386	243.99152
	B3	-487.45979	133.40379
	B4	107.64166	27.03348

I_{ON}/I_{OFF}	the concentration of hypochlorous acid (mmol/L)			the relative deviation	
	0 mm (A)	2 mm (B)	3 mm (C)	|(B-A)/A|	|(C-A)/A|
1	1.0125	1.015	1.02681	0.002469	0.014751
2	1.12046	1.11668	1.13898	0.003374	0.014126
3	1.20846	1.19897	1.23222	0.007853	0.014643
4	1.28147	1.26899	1.30837	0.009739	0.016048
5	1.34027	1.32741	1.36791	0.009595	0.018274
6	1.38762	1.37568	1.41479	0.008605	0.020222
7	1.42653	1.4159	1.45283	0.007452	0.02097
8	1.45931	1.45	1.48466	0.00638	0.020396
9	1.48754	1.47944	1.51199	0.005445	0.019206
10	1.51233	1.5053	1.53595	0.004648	0.017357
11	1.53443	1.52833	1.5573	0.003975	0.015131
12	1.55438	1.54909	1.57658	0.003403	0.014282
Average				0.006078	0.017381

Figure S12. The fitting equation and hypochlorous acid concentration calculated from the fitting equation. We assumed the ratio values are 1, 2, 3, 4……12.

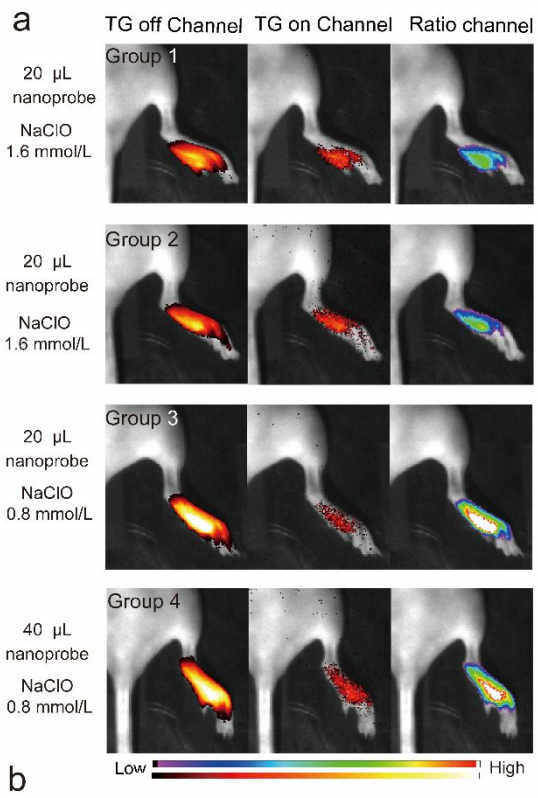

	$I_{TG\ off\ Channel}$ (counts)	$I_{TG\ on\ Channel}$ (counts)	$I_{off\ /\ on}$
1, (0mm)	33300	28000	1.2
2, (2 mm)	19800	16700	1.2
3, (3 mm)	16000	12000	1.3

Figure S13. (a) *In vivo* images of living mice with injection of different amount $NaYF_4$:Nd@Cy860@PC treated with different concentration of hypochlorite acid (gain 20, exposure time: TG on channel 10 s, TG off channel 5 s).(b) the summary of intensities of capillaries buried in mouse (TG on channel and TG off channel).

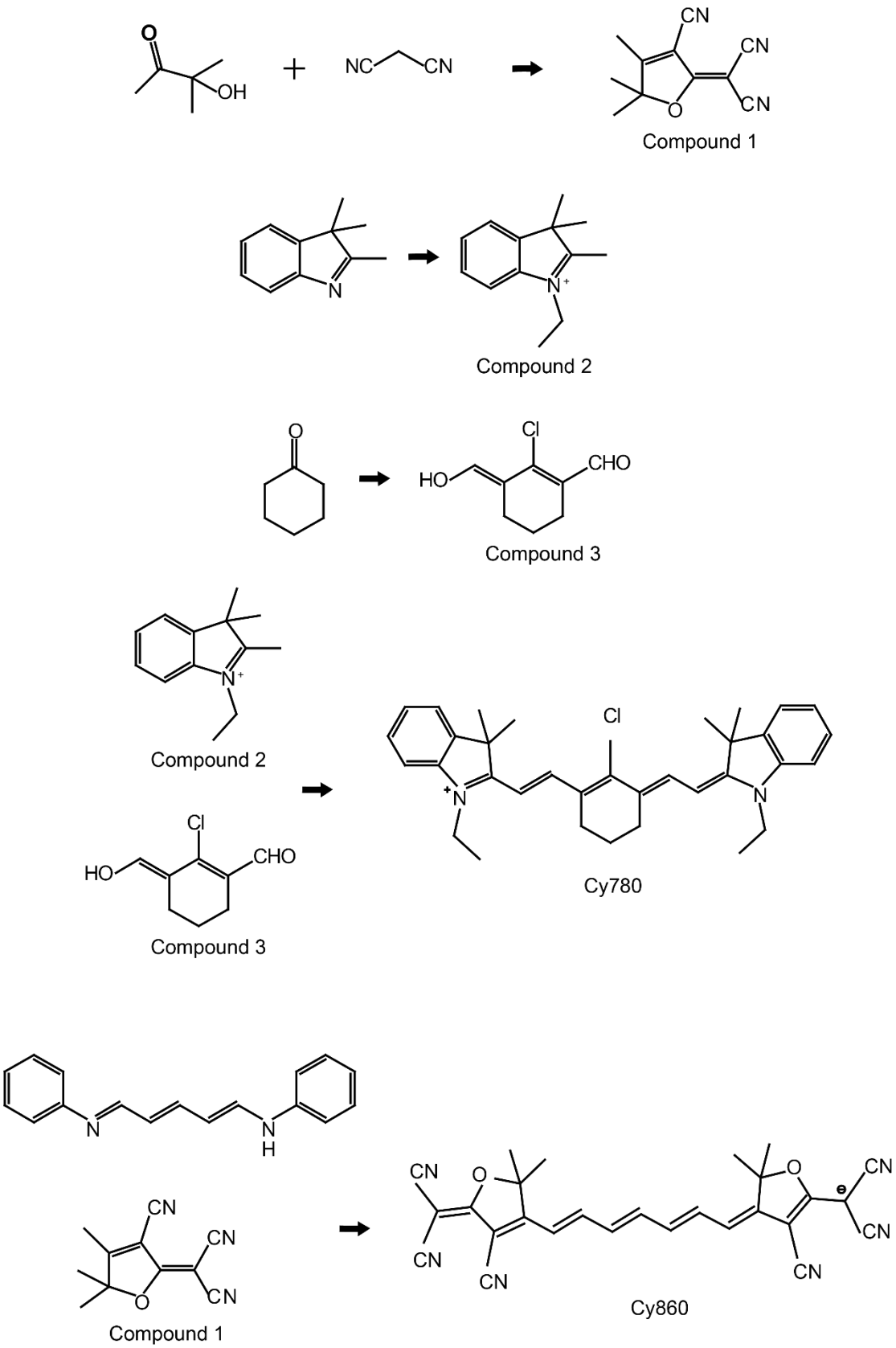

Figure S14. Synthetic route of the compound 1,compound 2, compound 3, Cy780 and Cy860.

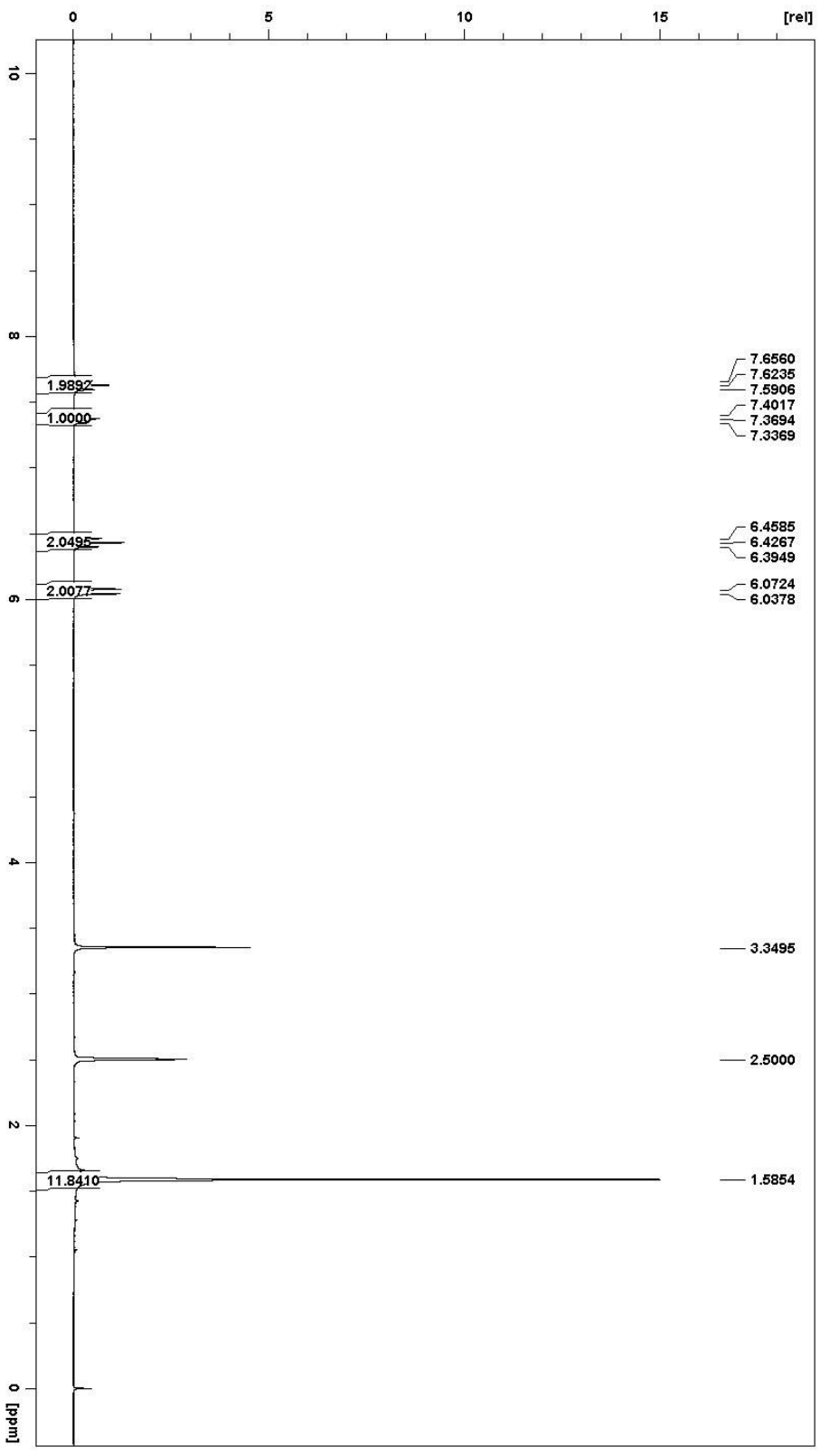

Figure S15.^{1}H NMR spectra of compound Cy860 in DMSO

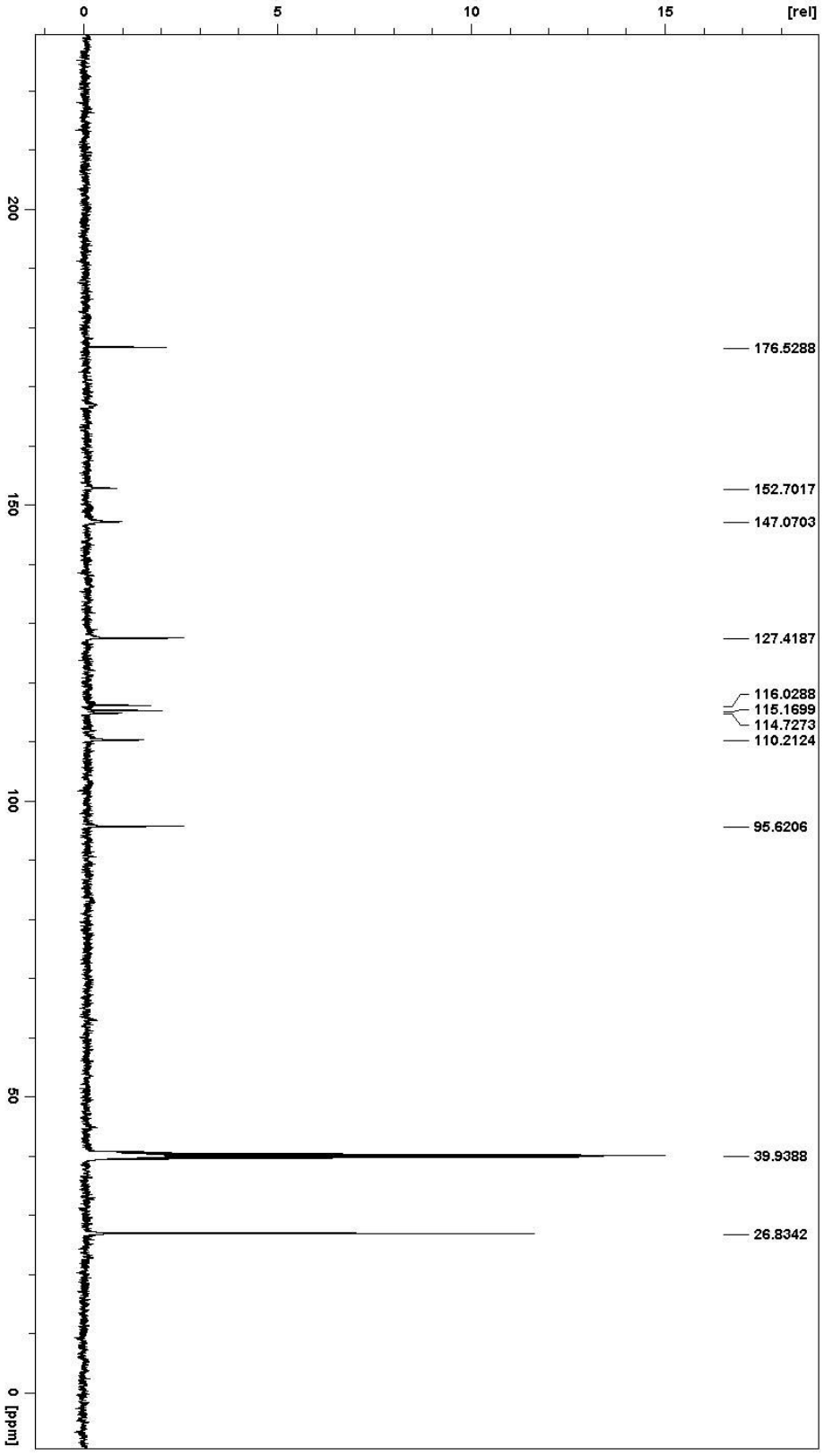

Figure S16.^{13}C NMR spectrum of compound Cy860 in DMSO

REFERENCES

(1) Ishimaru, A. Transport theory of waves in randomly distributed scatterers.

In *Wave Propagation and Scattering in Random Media*, 2nd ed.; Dudley, D., Ed.; IEEE/OU Press: New York, 1997; pp 145-166.
(2) Niemz, M. H. Light and matter. In *Laser-Tissue Interactions*, 3rd ed.; Greenbaum, E., Ed.; Springer-Verlag Berlin Heidelberg Press: Berlin, Heidelberg, 2003; pp 9-35.